Relativistic calculation of atomic M-shell ionization by protons

Mau Hsiung Chen and Bernd Crasemann
Department of Physics and Chemical Physics Institute, University of Oregon, Eugene, Oregon 97403

Hans Mark
National Aeronautics and Space Administration, Washington, D.C. 20546

(Received 6 December 1982)

Relativistic plane-wave Born-approximation calculations of cross sections for M-shell ionization of $_{67}$Ho, $_{79}$Au, and $_{92}$U by protons with incident energies from 0.05 to 1 MeV are reported. Dirac-Hartree-Slater wave functions were employed and binding-energy change and Coulomb deflection were taken into account. Associated x-ray production cross sections were also computed. Results are compared with previous theoretical predictions and with experimental data. Definite improvement in the theory has been attained by the use of realistic wave functions and consistent inclusion of the effects of relativity.

I. INTRODUCTION

Atomic inner-shell ionization by charged-particle impact has been subject to intensive studies during recent years. The theory has progressed beyond the plane-wave Born approximation by incorporation of binding and Coulomb-deflection effects.[1,2] The effects of relativity and of the choice of more realistic than hydrogenic wave functions were found to be quite important for low-energy collisions.[3–6] Most studies were limited, however, to K- and L-shell ionization. Only few measurements have been made of M-shell ionization because the M x-ray spectrum is so complex. Except for the early work of Jopson *et al.*,[7] the first of these measurements dealt with incident-ion energies of 1 MeV/u or higher.[8–15] Only recently have experimental data become available on M x-ray production cross sections under low-energy ion impact.[16,17] These data are valuable for the study of binding and Coulomb corrections, and relativistic and wave-function effects. On the theoretical side, calculations of M-shell ionization cross sections have been carried out in the plane-wave Born approximation with screened hydrogenic wave functions.[18,19] Going beyond the first Born approximation, the perturbed-stationary-state approach including energy loss, Coulomb deflection, and relativistic effects has been extended to the calculation of M-shell ionization cross sections[17]; the effects of relativity were estimated through a phenomenological approach.[20] The effect of wave functions on M-shell ionization cross sections was recently shown to be very important for medium-Z atoms.[21] As yet, however, there has been no truly relativistic calculation of M-shell ionization cross sections.

In order to look into the effects of more realistic wave functions and of a consistent incorporation of relativity, we have extended our relativistic Dirac-Hartree-Slater calculations of L-shell ionization cross sections[4] to the M shell. Here we report on results for M-shell ionization of $_{67}$Ho, $_{79}$Au, and $_{92}$U by protons with incident energies from 0.05 to 1 MeV.

II. THEORY

In the plane-wave Born approximation (PWBA),[1] the differential cross section for ejection of an electron from a closed atomic n shell by heavy-charged-particle impact is

$$\frac{d\sigma}{dE_f}=\frac{4\pi}{\hbar^2}Z_1^2e^4\frac{M_1}{E_1}(2j_n+1)\int_{q_{\min}}^{q_{\max}}\frac{dq}{q^3}\,|F_{fi}(q)|^2 \ . \qquad (1)$$

Here, E_f is the kinetic energy of the ejected electron, $\hbar\vec{q}$ is the momentum transferred to that electron, and Z_1, M_1, and E_1 are the charge, mass, and initial kinetic energy of the projectile, respectively. The exact limits of the momentum transfer[2,4] were used in the present calculation.

For an atomic shell with quantum numbers l_i, j_i, the relativistic form factor pertaining to the $l_f j_f$ partial wave is

$$|F_{fi}(q)|^2=\sum_{l=0}^{\infty}(2l+1)(2j_f+1)\begin{pmatrix} j_f & l & j_i \\ \frac{1}{2} & 0 & -\frac{1}{2}\end{pmatrix}^2 \Pi(l_f l l_i)\left|\int j_l(qr)(G_iG_f^*+F_iF_f^*)dr\right|^2 \ , \qquad (2)$$

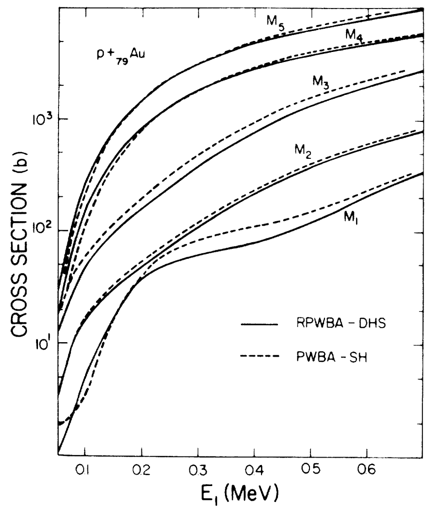

FIG. 1. Cross sections for M_i-subshell ionization of Au by proton bombardment, as functions of incident-proton energy. Results of the present relativistic plane-wave Born-approximation calculations from Dirac-Hartree-Slater wave functions (RPWBA-DHS) are compared with cross sections computed nonrelativistically from screened hydrogenic wave functions (PWBA-SH) (Ref. 19).

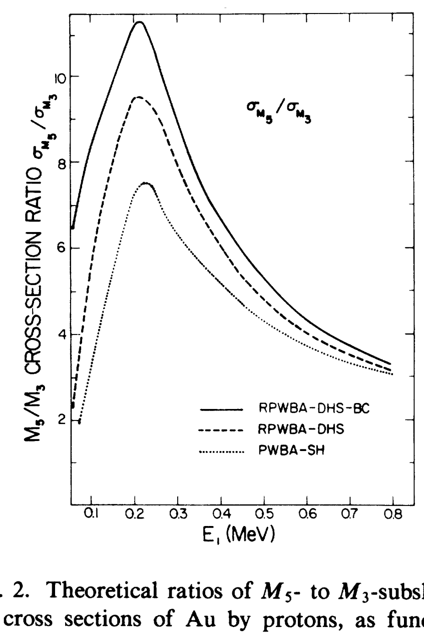

FIG. 2. Theoretical ratios of M_5- to M_3-subshell ionization cross sections of Au by protons, as functions of incident-proton energy. Present RPWBA results from DHS wave functions, with binding-energy and Coulomb-deflection corrections (RPWBA-DHS-BC) and without these corrections (RPWBA-DHS), are compared with nonrelativistic cross sections computed from screened hydrogenic wave functions (PWBA-SH) (Ref. 19).

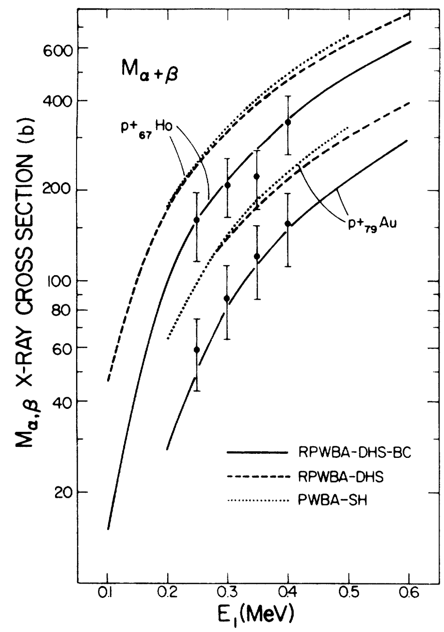

FIG. 3. Cross sections for the production of $M\alpha+\beta$ x rays from M-shell ionization of Ho and Au by protons, as functions of incident-proton energy. Theoretical results from the present relativistic calculations with binding-energy and Coulomb-deflection corrections (RPWBA-DHS-BC) and without these corrections (RPWBA-DHS), and from nonrelativistic calculations with screened hydrogenic wave functions (PWBA-SH) (Ref. 19), are compared with experimental data from Ref. 16.

where

$$\Pi(l_f l l_i)=\begin{cases}0 & \text{if } l_f+l+l_i=\text{odd}\\ 1 & \text{if } l_f+l+l_i=\text{even}\end{cases} \tag{3}$$

and G and F are the large and small components of the relativistic one-electron wave function.

In a classical representation, the binding energy of an atomic electron to be ionized is increased due to the presence of the slow charged projectile in the vicinity of the nucleus during the collision. This perturbation of the target atomic states by the projectile leads to a reduction in ionization probability. To take into account this binding effect, the M-shell binding energies of the united atom (i.e., of the atom with atomic number Z_2+1 in the case of proton impact) were used in the present calculations.

In the semiclassical approximation, the effect of the Coulomb repulsion between the projectile and target nucleus on the inner-shell ionization can be taken into account by applying a correction factor to the cross section calculated for a straight-line projectile path.[22,23] Including the Coulomb-deflection correction factors, the differential cross sections can be expanded as follows[22,23]:

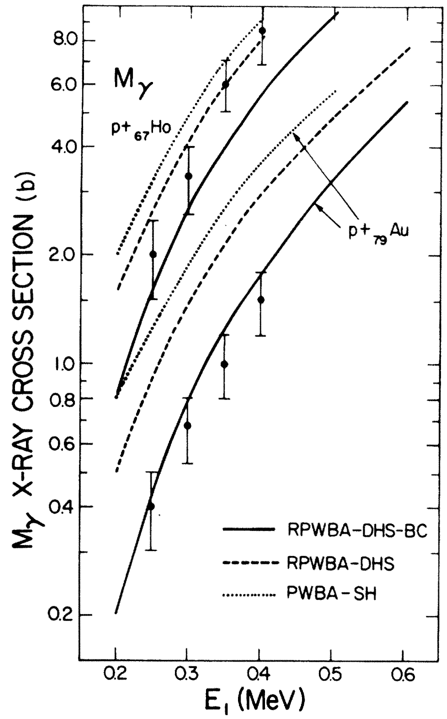

FIG. 4. Cross sections for the production of $M\gamma$ x rays from M-shell ionization of Ho and Au by protons, as functions of incident-proton energy. Theoretical results from the present relativistic calculations with binding-energy and Coulomb-deflection corrections (RPWBA-DHS-BC) and without these corrections (RPWBA-DHS), and from nonrelativistic calculations with screened hydrogenic wave functions (PWBA-SH) (Ref. 19), are compared with experimental data from Ref. 16.

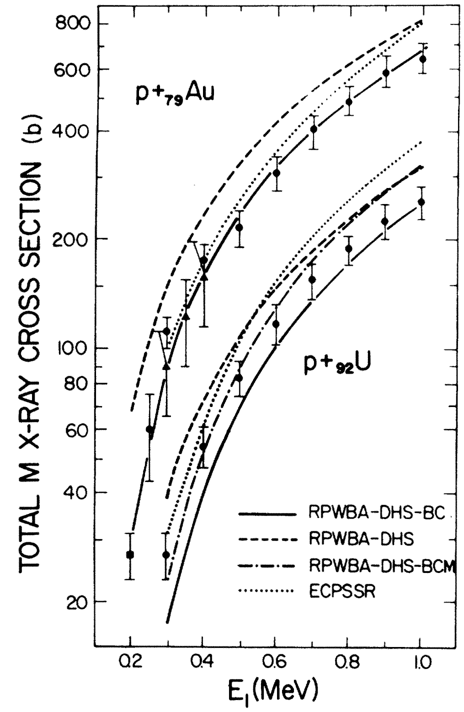

FIG. 5. Total M x-ray production cross sections for M-shell ionization of Au and U by protons, as functions of incident-proton energy. Theoretical curves are as follows. RPWBA-DHS-BC, present relativistic calculations including binding-energy and Coulomb-deflection corrections; RPWBA-DHS, same, without these corrections; RPWBA-DHS-BCM, present relativistic calculations with binding and Coulomb corrections, employing McGuire's fluorescence and Coster-Kronig yields (Ref. 29) instead of relativistic yields (Ref. 27); ECPSSR, calculations of Mehta *et al.* (Ref. 17) including energy-loss and Coulomb-deflection corrections, from the perturbed-stationary-state approach, with screened hydrogenic wave functions and relativistic corrections. Experimental data are from Refs. 16 and 17.

$$\left[\frac{d\sigma_n}{dE_f}\right]^C = \left[\frac{d\sigma_n}{dE_f}\right]^{\mathrm{PWBA}} \exp(-\pi d q_0) \ , \qquad (4)$$

where we have

$$q_0 = (U_n + E_f)/v_1 \ . \qquad (5)$$

U_n is the binding energy of an n-shell electron, and d is the half-distance between the collision partners at closest approach. In the present calculations, Eq. (4) was used to incorporate the Coulomb-deflection effect in the relativistic plane-wave cross section.

III. NUMERICAL METHOD

A general computer program, written for calculating relativistic PWBA (RPWBA) ionization cross sections with Dirac-Hartree-Slater (DHS) wave functions[4] was employed to evaluate the M_i-subshell Coulomb ionization cross sections. The atomic form factors were calculated with DHS wave functions[24,25] that describe the neutral atom. The continuum wave functions were found by solving the DHS equations in the same atomic potential as for the initial state. The spherical Bessel transformation of Eq. (2) was carried out with a technique developed by Talman.[26] Taking a logarithmic mesh in position and momentum spaces, the form-factor integral could be evaluated by two successive fast Fourier transforms.[26] The detailed numerical procedure is described in Ref. 4.

IV. RESULTS AND DISCUSSION

The present theoretical RPWBA-DHS cross sections with and without binding and Coulomb corrections for M_i-subshell ($i=1$—5) ionization of $_{67}$Ho, $_{79}$Au, and $_{92}$U by protons with E_1 between 0.05 and 1.0 MeV are listed in Table I. In Fig. 1, our present RPWBA-DHS cross sections for Au are compared

TABLE I. Relativistic plane-wave Born-approximation cross sections (RPWBA) (in barns), calculated from Dirac-Hartree-Slater wave functions for M-subshell ionization of Ho, Au, and U by protons of energy E_1 (in MeV). RPWBA-BC is the same as RPWBA but with binding-energy and Coulomb corrections. Numbers in parentheses indicate powers of 10, e.g., $9.14(-2)=9.14\times10^{-2}$.

	M_1		M_2		M_3		M_4		M_5	
E_1	RPWBA	RPWBA-BC	RPWBA	RPWBA-BC	RPWBA	RPWBA-BC	RPWBA	RPWBA-BC	RPWBA	RPWBA-BC
					$_{67}$Ho					
0.05	6.44	9.14(−2)	2.78(1)	6.84(−1)	7.88(1)	2.68	2.62(2)	1.66(1)	4.56(2)	3.11(1)
0.1	6.37(1)	1.31(1)	8.81(1)	1.97(1)	2.46(2)	6.19(1)	1.61(3)	5.13(2)	2.78(3)	9.16(2)
0.2	1.59(2)	8.44(1)	3.70(2)	1.83(2)	1.15(3)	6.05(2)	5.92(3)	3.54(3)	9.75(3)	5.91(3)
0.3	2.88(2)	1.69(2)	9.99(2)	6.13(2)	3.06(3)	1.97(3)	1.05(4)	7.44(3)	1.70(4)	1.22(4)
0.4	7.10(2)	4.37(2)	1.94(3)	1.32(3)	5.76(3)	4.08(3)	1.49(4)	1.14(4)	2.41(4)	1.86(4)
0.5	1.46(3)	9.69(2)	3.09(3)	2.25(3)	8.92(3)	6.70(3)	1.91(4)	1.52(4)	3.11(4)	2.49(4)
0.6	2.45(3)	1.73(3)	4.35(3)	3.30(3)	1.23(4)	9.62(3)	2.31(4)	1.89(4)	3.78(4)	3.10(4)
0.7	3.58(3)	2.65(3)	5.65(3)	4.42(3)	1.57(4)	1.27(4)	2.69(4)	2.25(4)	4.41(4)	3.68(4)
0.8	4.80(3)	3.68(3)	6.95(3)	5.57(3)	1.90(4)	1.57(4)	3.06(4)	2.59(4)	5.01(4)	4.25(4)
0.9	6.03(3)	4.76(3)	8.17(3)	6.69(3)	2.22(4)	1.86(4)	3.39(4)	2.90(4)	5.56(4)	4.77(4)
1.0	7.22(3)	5.83(3)	9.36(3)	7.78(3)	2.52(4)	2.14(4)	3.72(4)	3.21(4)	6.08(4)	5.26(4)
					$_{79}$Au					
0.05	1.10	4.61(−4)	3.27	3.85(−3)	1.26(1)	3.40(−2)	1.49(1)	1.02(−1)	2.70(1)	2.18(−1)
0.1	5.33	2.90(−1)	1.55(1)	1.13	4.77(1)	4.72	1.48(2)	2.04(1)	2.71(2)	3.99(1)
0.2	3.85(1)	1.27(1)	4.79(1)	1.60(1)	1.57(2)	5.89(1)	8.33(2)	3.58(2)	1.49(3)	6.62(2)
0.3	6.18(1)	3.25(1)	1.09(2)	5.32(1)	3.94(2)	2.08(2)	1.81(3)	1.06(3)	3.10(3)	1.86(3)
0.4	7.81(1)	4.75(1)	2.17(2)	1.25(2)	7.93(2)	4.87(2)	2.85(3)	1.92(3)	4.76(3)	3.26(3)
0.5	1.20(2)	7.32(1)	3.74(2)	2.37(2)	1.34(3)	8.99(2)	3.87(3)	2.81(3)	6.41(3)	4.71(3)
0.6	2.07(2)	1.28(2)	5.75(2)	3.88(2)	2.01(3)	1.43(3)	4.86(3)	3.71(3)	8.04(3)	6.17(3)
0.7	3.47(2)	2.23(2)	8.13(2)	5.73(2)	2.76(3)	2.04(3)	5.83(3)	4.58(3)	9.66(3)	7.64(3)
0.8	5.34(2)	3.58(2)	1.08(3)	7.86(2)	3.58(3)	2.73(3)	6.76(3)	5.44(3)	1.12(4)	9.08(3)
0.9	7.59(2)	5.29(2)	1.36(3)	1.02(3)	4.42(3)	3.46(3)	7.69(3)	6.29(3)	1.28(4)	1.05(4)
1.0	1.01(3)	7.31(2)	1.65(3)	1.27(3)	5.29(3)	4.22(3)	8.57(3)	7.11(3)	1.43(4)	1.19(4)
					$_{92}$U					
0.1	6.04(−1)	2.70(−3)	2.02	1.97(−2)	8.58	1.77(−1)	9.82	3.37(−1)	1.85(1)	7.39(−1)
0.2	4.14	5.82(−1)	8.60	1.40	2.90(1)	6.25	8.83(1)	2.29(1)	1.73(2)	4.75(1)
0.3	1.27(1)	4.15	1.61(1)	5.44	5.85(1)	2.31(1)	2.49(2)	1.10(2)	4.79(2)	2.20(2)
0.4	2.07(1)	9.72	2.63(1)	1.20(1)	1.08(2)	5.55(1)	4.67(2)	2.60(2)	8.63(2)	4.96(2)
0.5	2.55(1)	1.46(1)	4.18(1)	2.23(1)	1.85(2)	1.09(2)	7.14(2)	4.53(2)	1.27(3)	8.30(2)
0.6	2.91(1)	1.83(1)	6.38(1)	3.76(1)	2.89(2)	1.85(2)	9.71(2)	6.69(2)	1.69(3)	1.19(3)
0.7	3.45(1)	2.25(1)	9.26(1)	5.83(1)	4.19(2)	2.86(2)	1.23(3)	8.92(2)	2.11(3)	1.56(3)
0.8	4.48(1)	2.92(1)	1.29(2)	8.50(1)	5.72(2)	4.07(2)	1.48(3)	1.12(3)	2.52(3)	1.93(3)
0.9	6.18(1)	4.03(1)	1.72(2)	1.18(2)	7.47(2)	5.49(2)	1.72(3)	1.34(3)	2.93(3)	2.30(3)
1.0	8.66(1)	5.69(1)	2.21(2)	1.56(2)	9.38(2)	7.08(2)	1.97(3)	1.57(3)	3.34(3)	2.68(3)

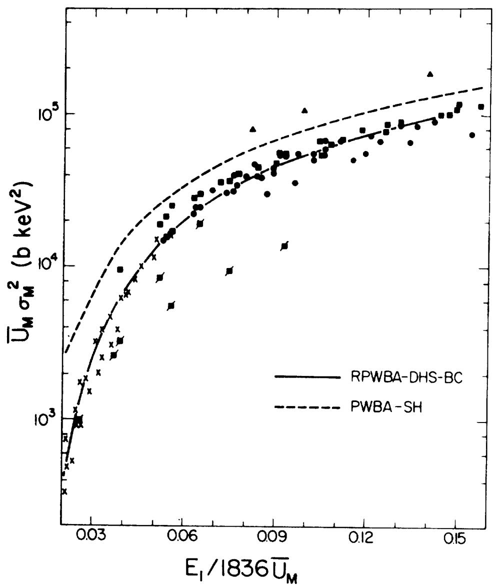

FIG. 6. Approximate universal curve (see text) of predicted and measured cross sections for the production of M x rays by M-shell ionization with protons. Curve denoted by RPWBA-DHS-BC is the prediction of the present relativistic calculations with binding and Coulomb corrections; PWBA-SH is the curve derived from nonrelativistic calculations with screened hydrogenic wave functions (Ref. 19). Experimental results are from Ref. 7 (slashed solid squares), Ref. 8 (crosses), Ref. 9 (solid triangles), Ref. 16 (solid circles), and Ref. 17 (solid squares).

with PWBA results from nonrelativistic screened hydrogenic (SH) wave functions.[19] For M_4- and M_5-subshell cross sections with projectile energies $50 \leq E_1 \leq 200$ keV, our present RPWBA-DHS results are larger by 10—50% than the PWBA-SH cross sections.[19] For the M_2 and M_3 subshells, our RPWBA-DHS results are smaller than the PWBA-SH cross sections by 10—20% in the range $50 \leq E_1 \leq 700$ keV. The inflection in the σ_{M_1} curve (Fig. 1) can be explained as a result of the generalized oscillator strength going through a minimum in the region $200 < E_1 < 500$ keV. In this energy region, σ_{M_1} is very sensitive to the atomic model because of strong cancellation in the atomic form factor.

Use of Hartree-Slater (HS) wave functions instead of SH wave functions has been found to reduce the M-shell ionization cross sections for medium-Z atoms.[21] The effect of relativity tends to increase the cross sections.[4–6] A partial cancellation between wave-function effect and relativistic effect might therefore occur in our present DHS calculations. It would be interesting to separate these two effects by making distinct HS and DHS calculations and comparing the results.

In Fig. 2, we compare the $\sigma_{M_5}/\sigma_{M_3}$ ionization cross-section ratios for Au from various theoretical approaches. The ratios from DHS calculations exceed those from SH calculations by as much as a factor of 2. Comparison with experimental ratios would thus provide a sensitive test of theory, but the requisite data do not yet exist in the literature.

There are two primary modes of vacancy production in the target atom by heavy-ion collision: (1) direct Coulomb ionization to the target continuum and (2) electron capture by the projectile. The contribution from electron capture to the cross sections for ionization of heavy target atoms by protons has been found to be less than 3.4% for incident energies $0.3 \leq E_1 \leq 2.6$ MeV,[17] which is well within the experimental error in the cross sections. In the present work, the contribution of electron capture to the M-shell ionization cross sections is not included in the calculations.

To compare experimental M x-ray cross sections[16] with theories, the various theoretical M-subshell ionization cross sections must be converted into $M\alpha$ (M_5-$N_{6,7}$), $M\beta$ (M_4-N_6), and $M\gamma$ ($M_3-N_{4,5}$) x-ray production cross sections,[16] using M-subshell fluorescence yields ω_i, Coster-Kronig yields[27] f_{ij}, and radiative widths.[28] If fluorescence and Coster-Kronig yields from McGuire's work[29] are used instead of our relativistic results,[27] the $M\alpha+\beta$ cross sections are changed by only $\sim 1\%$ while the $M\gamma$ cross sections are reduced by 10—15% for $_{67}$Ho and $_{79}$Au bombarded with protons. In Figs. 3 and 4, theoretical $M\alpha+\beta$ and $M\gamma$ cross sections of Ho and Au are compared with experimental measurements. The PWBA calculations from SH wave functions[19] overestimate the cross sections. Good agreement is found between experiment and the present RPWBA-DHS calculations including binding and Coulomb corrections.

Theoretical total M x-ray production cross sections were calculated from M-subshell ionization cross sections, fluorescence and Coster-Kronig yields,[27,29] and the relationship between x-ray production and ionization cross sections given in Ref. 19. In Fig. 5, theoretical total M x-ray production cross sections are compared with experimental measurements.[16,17] Excellent agreement is found between experimental results[16,17] and those of the present RPWBA-DHS calculations with binding and Coulomb corrections, for the case of Au ionized by protons. For the ionization of U by protons, the present theoretical M x-ray production cross sections are too low at low bombarding energy (by $\sim$15—25%) if fluorescence and Coster-Kronig yields from Ref. 27 are used, while they are too high at higher bombarding energies (by $\sim$10—25%) if fluorescence and Coster-Kronig yields from Ref. 29

are used.

Theoretical M x-ray production cross sections from the perturbed-stationary-state approach including energy loss, Coulomb deflection, and relativistic corrections have been computed by Mehta *et al.* with screened hydrogenic wave functions and McGuire's fluorescence and Coster-Kronig yields.[29] The results of these calculations[17] exceed those of our present RPWBA-DHS calculations with binding and Coulomb corrections by $\sim$10–20%. Compared with experiment, the calculations of Mehta *et al.*[17] overestimate the M x-ray production cross sections for Au and U under bombardment with protons of $E_1 > 400$ keV. The better wave functions and *ab initio* inclusion of relativity in the present computations cause a definite improvement in the agreement between theory and experiment.

An approximate universal curve for all the experimental M x-ray production cross sections can be obtained by plotting $U_M^2 \sigma_M$ as a function of $E_1/\bar{U}_M$. Here, $\bar{U}_M$ is the average M-shell binding energy,

$$\bar{U}_M = \sum_{i=1}^{5} \tfrac{1}{18} N_{M_i} U_{M_i} \qquad (6)$$

with N_{M_i} electrons in the M_i subshell in which the binding energy is U_{M_i}.[16] The total ionization cross section σ_M is related to the total M x-ray production cross section σ_{Mx} through

$$\sigma_M = \sigma_{Mx} / \bar{\omega}_M \ , \qquad (7)$$

where $\bar{\omega}_M$ is the average M-shell fluorescence yield

$$\bar{\omega}_M = \sum_{i=1}^{5} \tfrac{1}{18} N_{M_i} \nu_i \ , \qquad (8)$$

ν_i being the total number of characteristic M-shell x rays (not necessarily from the radiative filling of an M_i-subshell vacancy) that result per primary vacancy in the M_i subshell.[30] The "effective fluorescence yields" ν_i are related to the M-subshell fluorescence yields ω_i and Coster-Kronig yields f_{ij} through Eq. (1-17) of Ref. 30. We calculated the average fluorescence yields $\bar{\omega}_M$ from Eq. (8) with the M-subshell fluorescence and Coster-Kronig yields from DHS-model theory.[27] In Fig. 6, the approximate universal curve from experiment is compared with theoretical predictions. The results from PWBA calculations with SH wave functions[19] appear to be consistently larger than experiment. The present RPWBA-DHS predictions including binding and Coulomb corrections, on the other hand, seem to agree quite well with the majority of experimental data.

ACKNOWLEDGMENT

This work was supported in part by the U. S. Air Force Office of Scientific Research under Grant No. AFOSR-79-0026.

[1] D. H. Madison and E. Merzbacher, in *Atomic Inner-Shell Processes,* edited by B. Crasemann (Academic, New York, 1975), Vol. 1, p. 1.

[2] W. Brandt and G. Lapicki, Phys. Rev. A 23, 1717 (1981).

[3] G. Lapicki and A. R. Zander, Phys. Rev. A 23, 2072 (1981).

[4] M. H. Chen, B. Crasemann, and H. Mark, Phys. Rev. A 26, 1243 (1982).

[5] T. Mukoyama and L. Sarkadi, Phys. Rev. A 23, 375 (1981).

[6] T. Mukoyama and L. Sarkadi, Phys. Rev. A 25, 1411 (1982).

[7] R. C. Jopson, H. Mark, and C. D. Swift, Phys. Rev. 127, 1612 (1962).

[8] P. B. Needham, Jr. and B. D. Sartwell, Phys. Rev. A 2, 27 (1970); 2, 1686 (1971).

[9] C. E. Busch, A. B. Baskin, P. H. Nettles, S. M. Shafroth, and A. W. Waltner, Phys. Rev. A 7, 1601 (1973).

[10] S. T. Thornton, R. H. McKnight, and R. R. Karlowicz, Phys. Rev. A 10, 219 (1974).

[11] K. Ishii, S. Morita, H. Tawara, H. Kaji, and T. Shiokawa, Phys. Rev. A 11, 119 (1975).

[12] V. S. Nikolaev, V. P. Petukhov, E. A. Romanovsky, V. A. Sergeev, I. M. Kruglova, and V. V. Beloshitsky, in *The Physics of Electronic and Atomic Collisions,* edited by J. S. Risley and R. Geballe (University of Washington Press, Seattle, 1975), p. 419.

[13] M. Poncet and Ch. Engelman, Nucl. Instrum. Methods 159, 455 (1979).

[14] H. J. Hay, J. Soderbaum, and P. B. Treacy, Nucl. Instrum. Methods 170, 261 (1980).

[15] K. Sera, K. Ishii, A. Yamadera, A. Kuwako, M. Kamiya, M. Sebata, S. Morita, and T.-C. Chu, Phys. Rev. A 22, 2536 (1980).

[16] M. Sarkar, H. Mommsen, W. Sarter, and P. Schurkes, J. Phys. B 14, 3163 (1981).

[17] M. Mehta, J. L. Duggan, J. L. Price, F. D. McDaniel, and G. Lapicki, Phys. Rev. A 26, 1883 (1982).

[18] B.-H. Choi, Phys. Rev. A 7, 2056 (1973).

[19] D. E. Johnson, G. Basbas, and F. D. McDaniel, At. Data Nucl. Data Tables 24, 1 (1979).

[20] W. Brandt and G. Lapicki, Phys. Rev. A 20, 465 (1979).

[21] V. V. Sizov and N. M. Kabachnik, J. Phys. B 14, 2013 (1981).

[22] J. Bang and J. M. Hansteen, K. Dan. Vidensk. Selsk. Mat.—Fys. Medd. 31, No. 13 (1959).

[23] G. Basbas, W. Brandt, and R. Laubert, Phys. Rev. A 7, 983 (1973).

[24] D. A. Liberman, D. T. Cromer, and J. T. Waber, Comput. Phys. Commun. 2, 107 (1971).

[25] K.-N. Huang, M. Aoyagi, M. H. Chen, B. Crasemann, and H. Mark, At. Data Nucl. Data Tables 18, 243 (1976).
[26] J. D. Talman, J. Comput. Phys. 29, 35 (1978).
[27] M. H. Chen, B. Crasemann, and H. Mark, Phys. Rev. A 21, 449 (1980) and unpublished.
[28] C. P. Bhalla, J. Phys. B 3, 916 (1970).
[29] E. J. McGuire, Phys. Rev. A 5, 1043 (1972).
[30] W. Bambynek, B. Crasemann, R. W. Fink, H.-U. Freund, H. Mark, C. D. Swift, R. E. Price, and P. Venugopala Rao, Rev. Mod. Phys. 44, 716 (1972).